

**ПАРАМЕТРЫ ПЛАЗМЫ И КОНЦЕНТРАЦИЯ АТОМОВ ФТОРА В СМЕСИ SF₆ + Ar + He:
ВЛИЯНИЕ СООТНОШЕНИЯ Ar/He, ДАВЛЕНИЯ И ВКЛАДЫВАЕМОЙ МОЩНОСТИ****А.В. Мяконьких, В.О. Кузьменко, А.М. Ефремов, К.В. Руденко**

Андрей Валерьевич Мяконьких (ORCID 0000-0002-9547-1619), Виталий Олегович Кузьменко (ORCID 0000-0002-7861-215X), Константин Васильевич Руденко (ORCID 0000-0001-5009-7590)

Физико-технологический институт им. К.А. Валиева РАН, Нахимовский пр., 34, Москва, Российская Федерация, 117218

E-mail: miakonkikh@ftian.ru, kuzmenko@ftian.ru, rudenko@ftian.ru

Александр Михайлович Ефремов (ORCID 0000-0002-9125-0763)*

НИИ Молекулярной электроники, ул. Академика Валиева, 6/1, Зеленоград, Москва, Российская Федерация, 124460, Россия

E-mail: aefremov@niime.ru*

Исследовано влияние начального состава смеси, давления газа и вкладываемой мощности на электрофизические параметры и концентрацию атомов фтора в плазме SF₆ + Ar + He, возбуждаемой в реакторе индукционного типа на частоте 2 МГц. При совместном использовании диагностики плазмы с помощью зондов Ленгмюра и оптической эмиссионной спектроскопии определен характер и сделаны предположения о механизмах влияния варьируемых параметров на характеристики электронной и ионной компонент плазмы. В частности, показано, что замена аргона на гелий при постоянном содержании SF₆ влияет на температуру электронов, концентрации заряженных частиц и электроотрицательность плазмы через изменение суммарной скорости ионизации и потерь энергии электронов при их взаимодействии с доминирующими нейтральными частицами. Установлено, что максимальный эффект на концентрацию атомов фтора оказывает варьирование вкладываемой мощности (в ~ 9 раз при W = 800–1250 Вт), при этом влияние соотношения Ar/He и давления газа (особенно в области p < 15 мтор) выражены слабо. Причиной такой ситуации являются противоположные тенденции температуры и концентрации электронов, приводящие к малым изменениям эффективной частоты процессов вида SF_x + e → SF_{x-1} + F + e. Найдено, что плотности потоков атомов фтора (Γ_F) и положительных ионов (Γ₊) следуют изменениям концентраций соответствующих частиц, при том минимальные значения отношения Γ_F/Γ₊ в смесях с преобладающим содержанием He наблюдаются в области низких давлений и уровней вкладываемой мощности.

Ключевые слова: SF₆, плазма, параметры, активные частицы, ионизация, диссоциация

**PLASMA PARAMETERS AND FLUORINE ATOM DENSITY IN SF₆ + Ar + He GAS MIXTURE:
EFFECTS OF Ar/He MIXING RATIO, PRESSURE AND INPUT POWER****A.V. Miakonkikh, V.O. Kuzmenko, A.M. Efremov, K.V. Rudenko**

Andrey V. Miakonkikh (ORCID 0000-0002-9547-1619), Vitaly O. Kuzmenko (ORCID 0000-0002-7861-215X), Konstantin V. Rudenko (ORCID 0000-0001-5009-7590)

Valiev Institute of Physics and Technology RAS, Nahimovsky av., 34, Moscow, 117218, Russia

E-mail: miakonkikh@ftian.ru, kuzmenko@ftian.ru, rudenko@ftian.ru

Alexander M. Efremov (ORCID 0000-0002-9125-0763)*

Molecular Electronics Research Institute (MERI), Academic Valiev st., 6/1, Zelenograd, Moscow, 124460, Russia

E-mail: aefremov@niime.ru*

The influence of the initial mixture composition, gas pressure and input power on electro-physical parameters and density of fluorine atoms in SF₆ + Ar + He plasma produced in an inductive-type reactor at 2 MHz was investigated. The combination of plasma diagnostics by Langmuir probes and optical emission spectroscopy allowed one to determine behaviors of electrons- and ions-related plasma characteristics vs. variable operating parameters as well as to suggest mechanisms responsible for corresponding effects. In particular, it was shown that the substitution of argon by helium at constant SF₆ content in a feed gas affects the electron temperature, densities of charged species and plasma electronegativity through changes in both total ionization rate and electron energy losses during their interactions with dominant neutral particles. It was found that input power produces the maximum effect on the F atom density (by ~ 9 times at w = 800–1250 W) while the influence of the Ar/He ratio and gas pressure (especially at p < 15 mtorr) appears to be much weaker. Such situation is caused by opposite trends of electron temperature and electron density that results in rather small changes in the effective frequency of SF_x + e → SF_{x-1} + F + e reaction family. It was found that fluxes of both fluorine atoms (Γ_F) and positive ions (Γ₊) follow changes in their densities, and the minimum Γ_F/Γ₊ value in He-rich plasmas corresponds to low pressures and input powers.

Keywords: SF₆, plasma, parameters, active species, ionization, dissociation

Для цитирования:

Мяконьких А.В., Кузьменко В.О., Ефремов А.М., Руденко К.В. Параметры плазмы и концентрация атомов фтора в смеси SF₆ + Ar + He: влияние соотношения Ar/He, давления и вкладываемой мощности. *Изв. вузов. Химия и хим. технология*. 2025. Т. 68. Вып. 3. С. 42–49. DOI: 10.6060/ivkkt.20256803.7130.

For citation:

Miakonkikh A.V., Kuzmenko V.O., Efremov A.M., Rudenko K.V. Plasma parameters and fluorine atom density in SF₆ + Ar + He gas mixture: effects of Ar/He mixing ratio, pressure and input power. *ChemChemTech [Izv. Vyssh. Uchebn. Zaved. Khim. Khim. Tekhnol.]*. 2025. V. 68. N 3. P. 42–49. DOI: 10.6060/ivkkt.20256803.7130.

INTRODUCTION

Fluorine-containing gases have received numerous applications in modern microelectronic technology for the “dry” (plasma-assisted) etching/patterning of silicon and silicon-based materials [1, 2]. Among a variety of compounds used for these purposes, the leading role belongs to fluorocarbon gases with a general formula of C_xH_yF_z. From pervious etching experience, it can be concluded that their common feature is the deposition of fluorocarbon polymer film on any surfaces contacted with plasma [2-4], and the polymerization ability depends on the “z/x” ratio in the original molecule. Though the continuous thick film contaminates the treated wafer and lowers absolute etching rates, there are also some positive effects that allow one to obtain the advanced reactive-ion etching (RIE) characteristics. These are an improvement of etching anisotropy (as the polymer film protects side walls from the interaction with F atoms) as well as an increase in SiO₂/Si etching selectivity (as the thinner polymer film on the oxygen-containing surface does exist) [5-7].

At the same time, there are many plasma-etching-related tasks which assume the use of non-polymerizing source of fluorine atoms. The nearest exam-

ple is the SF₆ gas which does work in Bosch processes as well as in cryogenic etching processes (together with Ar and O₂) in order to provide the deep anisotropic patterning of silicon for micro-electro-mechanical systems (MEMS) [8, 9]. Except these, SF₆-based plasmas, and namely SF₆ + Ar gas mixtures, can also be used in conventional RIE processes which are not strongly focused on obtaining the anisotropic etching profile, but require both high etching rates at nearly room temperatures and decent surface clearness [3, 10, 11]. That is why there were several experimental and theoretical (model-based) works aimed at investigating physical and chemical properties of SF₆ [12, 13] and SF₆ + Ar [13-15] inductively-coupled plasmas under typical RIE conditions (gas pressures p < 20 mTorr, power densities w' > 0.01 W/cm³). In fact, the results of these studies allowed one to determine effects of processing on steady-state plasma parameters and densities of main active species, such as positive ions and F atoms, as well as to figure out gas-phase and heterogeneous reaction schemes providing obtained effects. In Refs. [13, 14], it was found also that the change in SF₆/Ar mixing ratio toward Ar-rich plasmas in less extent influences electron energy distribution function and electron temperature while exhibits the stronger effect on plasma density. The latter is probably because of sim-

ultaneous changes in total ionization rate and plasma electronegativity, as a decrease in densities of electro-negative species takes place.

On this background, the much less attention was paid to $\text{SF}_6 + \text{He}$ plasma, and there are no studies where the mixtures of SF_6 with Ar and He were compared under one and the same processing conditions. At the same time, the feature of He is high heat conductivity coefficient [16] that probably flattens gas temperature and density profiles due to the effective heat transfer from plasma to chamber walls. As an indirect confirmation, Ref. [17] reported that the addition of He to SF_6 causes the noticeable increase in plasma uniformity under the condition of dc glow discharge. Therefore, the study of relationships between operating conditions, electro-physical parameters and steady-state composition of $\text{SF}_6 + \text{He}$ plasma is an important task for the future progress in RIE technology.

With accounting for mentioned above, the general purpose of given work was to investigate physical and chemical properties of $\text{SF}_6 + \text{Ar} + \text{He}$ inductively-coupled plasma under typical RIE conditions. Accordingly, the topics of primary interest were a) to determine how the substitution of Ar by He influences electrons- and ions-related plasma parameters as well as the density of fluorine atoms; and b) to analyze the sensitivity of given plasma characteristics to changes in gas pressure and input power in He-rich gas mixtures.

EXPERIMENTAL DETAILS

Plasma diagnostics was performed in a PlasmaLab 100 (OIPT, UK) etch tool under the condition of inductively coupled RF (2 MHz) plasma [18, 19]. All experiments were carried out at constant total gas flow rate ($q = 120$ sccm) while variable operating parameters were input power ($w = 800\text{-}2750$ W), gas pressure ($p = 5\text{-}20$ mtorr) and initial composition of $\text{SF}_6 + \text{Ar} + \text{He}$ gas mixture. The given q value corresponded to the middle of nominal gas flow range for given reactor type as well as provided the nearly well-stirred operating regime. The first experimental series assumed the change in Ar/He mixing ratio at constant $p = 10$ mtorr and $w = 800$ W. In this case, the constant 60 sccm of SF_6 gas provided its fixed value of 50% while the remaining half was composed by various fractions of noble gases. Accordingly, an increase in q_{He} in the range of 0-55 sccm produced $y_{\text{He}} = 0\text{-}46\%$ together with a proportional decrease in y_{Ar} . The second and third experimental series were conducted in He-rich plasmas ($q_{\text{He}} = 50$ sccm that corresponded to $y_{\text{He}} = 42\%$) to study effects of gas pressure (at $w = 800$ W) and input power (at $p = 10$ mtorr).

In order to investigate the effect of operating parameters on electrons- and ions-related plasma characteristics, we applied plasma diagnostics by single RF-compensated Langmuir probe tool (Espion, Hiden Analytical, UK). The probe was installed through the viewport on the chamber wall, was located at ~ 11 cm above the bottom electrode used as the wafer holder as well as was centered in its radial position. The treatment of "raw" current-voltage (I-V) curves accounted for Maxwellian electron energy distribution function (EEDF) and was based on well-known statements of orbital motion limited (OML) theory for low pressure plasmas [20]. The corresponding procedure was carried out using the commercial software supplied by the equipment manufacturer. The effective ion mass, m^* , required as an input was roughly evaluated assuming SF_5^+ to be the dominant SF_6 -related positive ion [12]. Taking into account that ionization rate coefficients for both Ar and He atoms are sufficiently lower compared with that for SF_6 , the condition $y_{\text{Ar}} + y_{\text{He}} = 50\%$ means $m^* \approx \text{const}$. As outputs, we obtained electron temperature (T_e) total density of positive ions (n_+) and electron density (n_e). We would like to mention that Maxwellian EEDF is a widely used simplification for both plasma modeling and interpretation of experimental data related to low-pressure high-density inductive discharges [3], including SF_6 -based plasmas [12-15]. The physical reason is the sufficient contribution of equilibrium electron-electron collisions to the overall electron energy loss. As a confirmation, we obtained the nearly linear appearance of pure electron current in a semi-logarithmic scale.

Preliminary, we have conducted a series of experiments to determine the "plasma on" time resulting in the considerable degradation of probe tip. The criterion was the similarity of both raw voltage-current curves and related plasma parameters obtained for one and the same processing conditions. Accordingly, the tip was always replaced by the new one in prior to the "lifetime" expiration. After changing the tip, we repeated the previous point to be sure that there is no data shift. Each experimental point was reproduced by 5 times, and data were averaged before their plotting or further treatment. The typical deviation of experimental points obtained under identical processing conditions was about $\pm 5\%$.

In order to investigate the effect of operating parameters on steady-state densities of F atoms, we used optical emission spectroscopy (HR4 PRO, Ocean Insight, USA) in a combination with the actinometry method. The emission was taken through the sidewall viewport with the quartz window. The optical axis passed at ~ 10 cm below the Langmuir probe and at

~ 1 cm above the bottom electrode. Such a position corresponded to the quasi-neutral plasma region (in fact, to the identical condition with the Langmuir probe tool), but also provided the effective observation of reaction products during etching experiments. The focusing system prevented the shadowing effect from the electrode itself. Since our gas mixtures originally contained the known amount of Ar, we did not add the special reference gas, but monitored emission intensities for widely known actinometrical lines, Ar 750.4 nm and F 703.8 nm. The deviation of emission intensity data obtained under identical processing conditions was always below 10%. In fact, this couple has been successfully used by many researches because both excited states are definitely populated by the electron-impact excitation of ground-state atoms, are featured by known excitation cross-sections as well as exhibit the absolute domination of emissive relaxation pathways [21]. All these allow one to use the standard actinometrical approach in a form of

$$[F] = y_{\text{Ar}} N C_a (I_{\text{F}}/I_{\text{Ar}}), \quad (1)$$

where $N = p/k_{\text{B}}T_{\text{gas}}$ is the gas density at the temperature of T_{gas} , I_{F} and I_{Ar} are measured emission intensities, and $C_a = (\lambda_{\text{Ar}}k_{\text{ex,F}}A_{\text{F}})/(\lambda_{\text{F}}k_{\text{ex,Ar}}A_{\text{Ar}})$ is the actinometrical coefficient that depends on corresponding wavelengths (λ), excitation rate coefficients (k_{ex}) and optical transition probabilities (A). Excitation cross-sections for F and Ar atoms needed to calculate k_{ex} are available in Ref. [21]. From Ref. [21], it can be understood also that $C_a \approx \text{const}$ at $T_e = 3\text{--}6$ eV while F atom densities determined using the F 703.8 nm/Ar 750.4 nm intensity ratio are in acceptable agreement with mass-spectrometry experiments. The parameter T_{gas} was evaluated using the experimental data of Ref. [22] for pure SF_6 plasma with recalculations to actual levels of input power density and gas pressure. The dependence of T_{gas} on Ar/He mixing ratio was ignored. Similar approaches and procedure have been tested in our previous works dealt with fluorocarbon gas plasmas [23, 24].

RESULTS AND DISCUSSION

Fig. 1 illustrates how variable processing conditions influence electrons- and ions-related plasma parameters. As most of effects exhibit similar trends with those obtained for $\text{SF}_6 + \text{Ar}$ plasmas [13-15], below we provide only brief comments with attracting the attention on differences between Ar- and He-rich mixture conditions.

The substitution of Ar by He at constant SF_6 content in a feed gas causes the rather weak growth of electron temperature (Fig. 1(a)), but noticeably (by

~ 1.5 times at 0-46% He) lowers the electron density (Fig. 2(b)). In our opinion, the first phenomenon reasonably reflects the situation that a) He exhibits the lower momentum transfer cross-section ($\sim 4.5 \cdot 10^{-16}$ cm² compared with $\sim 1.3 \cdot 10^{-15}$ cm² for Ar at the incident electron energy of 10 eV), simply due to the lower effective atom size; and b) the first excitation potential for He atom (~ 19.8 eV) sufficiently exceeds that for Ar (~ 11.8 eV). Therefore, an increase in y_{He} lowers the electron energy loss in elastic collisions as well as shrinks the energy loss “window” for inelastic collisions that finally leads to an increase to mean electron energy. As for the second phenomenon, it directly originates from the change in total ionization rate. Really, from Refs. [25, 26], it can be concluded that reaction R1: $\text{He} + e \rightarrow \text{He}^+ + 2e$ is characterized by higher threshold energy (~ 24.6 eV) as well as exhibit the lower cross-section ($\sim 3.3 \cdot 10^{-17}$ cm² at the incident electron energy of 30 eV) compared with those for R2: $\text{Ar} + e \rightarrow \text{Ar}^+ + 2e$ (~ 15.8 eV and $\sim 1.8 \cdot 10^{-17}$ cm², respectively). That is why, as the Ar/He mixing ratio changes toward He-rich plasmas, the condition of $k_1 \ll k_2$ (for example, $2.8 \cdot 10^{-12}$ cm³/s for k_1 vs. $2.5 \cdot 10^{-10}$ cm³/s for k_2 at $T_e = 3$ eV) causes a rapid decrease in $k_1 y_{\text{He}} + k_2 y_{\text{Ar}}$ sum characterizing the joined contribution of noble gases in the total ionization rate. Accordingly, the latter also tends to decrease that reduces both electron production rate and electron density. From Fig. 1(c), it can be seen that the change of n_+ correlates with that for n_e , but appears to be much weaker in an absolute scale. This is due to decreasing efficiency of attachment processes, such as R3: $\text{SF}_6 + e \rightarrow \text{SF}_6^-$, R4: $\text{SF}_6 + e \rightarrow \text{SF}_5^- + \text{F}$ and R5: $\text{F}_2 + e \rightarrow \text{F} + \text{F}^-$, that retards the formation rate as well as reduces the density negative ions. At the same time, the n_+/n_e ratio characterizing plasma electronegativity demonstrates a weak growth toward higher y_{He} values (Fig. 1(d)).

An increase in gas pressure under the condition of $y_{\text{He}} > y_{\text{Ar}}$ and $w = \text{const}$ causes the simultaneous decrease in both electron temperature (Fig. 1(a)) and electron density (Fig. 1(b)). Obviously, the behavior of T_e represents a kind of standard response that does not depend on the type of gas environment. The reason is the growth of gas density, electron collision frequency and thus, of electron energy losses in both elastic and inelastic collisions. As for decreasing n_e , similar dependencies have been obtained in Ref. [12] in pure SF_6 gas by plasma modeling as well as in Ref. [15] in 50% $\text{SF}_6 + 50\%$ Ar gas mixture by the experiment. Such situation probably results from three parallel effects, and namely from a) decreasing ionization rate coefficients

for all neutral species together with T_e (for example, $4.7 \cdot 10^{-10}$ - $1.3 \cdot 10^{-10}$ cm^3/s for k_2 at 5-25 mtorr) that lowers the ionization efficiency; b) increasing electron losses in R3-R5 due to both reverse sensitivity of low-threshold k_3 - k_5 to the change in T_e (for example, $4.0 \cdot 10^{-11}$ - $5.5 \cdot 10^{-11}$ cm^3/s for k_3 at 5-25 mtorr) and increasing densities of electronegative fluorine-containing species; and c) providing more favorable conditions for the dif-

fusion of electrons toward chamber walls due to increasing plasma electronegativity, as shown in Fig. 1(d). The latter means, in fact, the transition from ambipolar to free diffusion mechanism. The density of positive ions also goes down following the change in total ionization rate. The same behavior is also for ion flux, $\Gamma_+ \approx 0.61n_+v_B$, as the ion Bohm velocity v_B accounts for T_e under the square root.

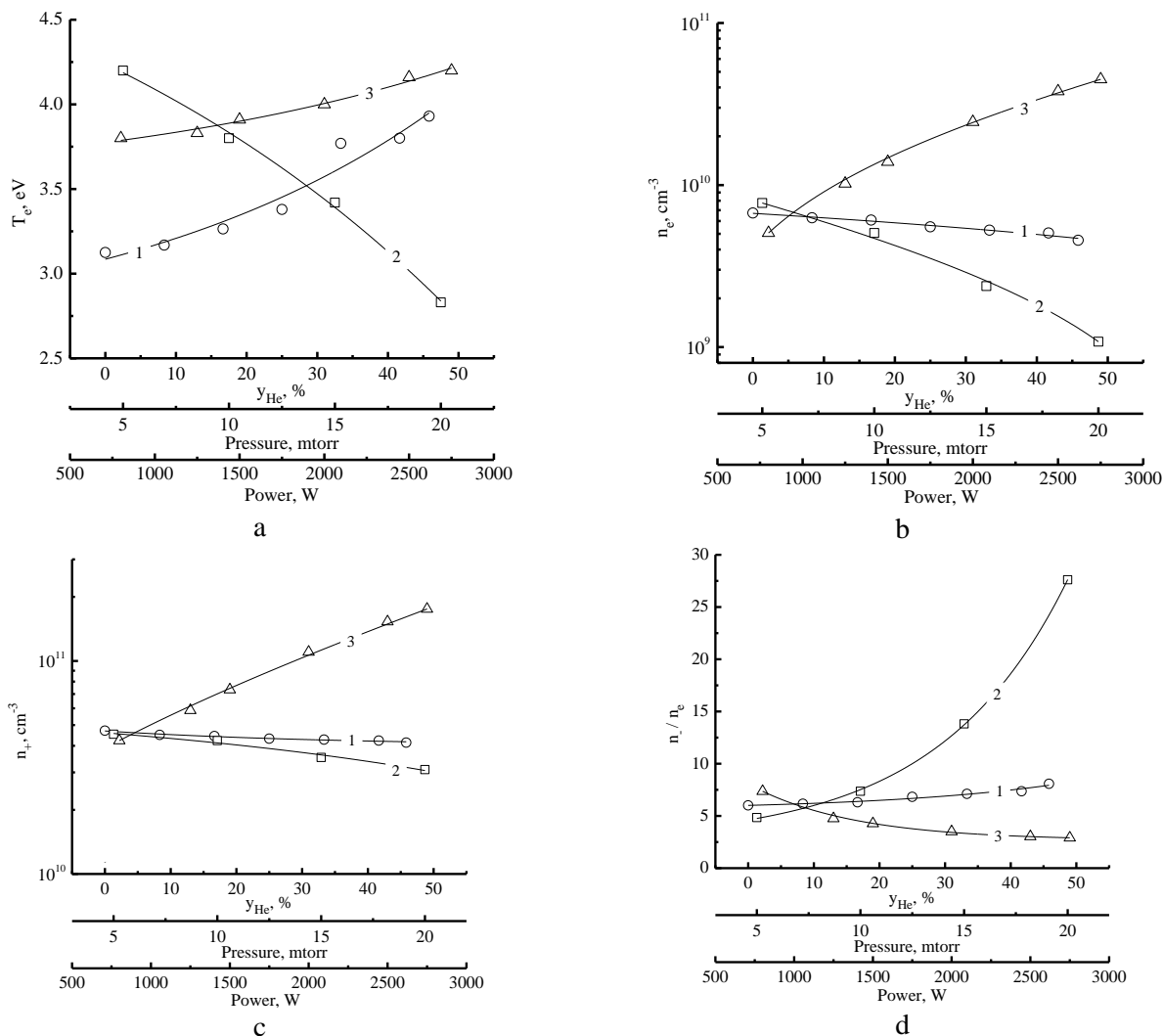


Fig. 1. Electrons- and ions-related plasma parameters as functions of He fraction in a feed gas (1, at $p = 10$ mtorr and $w = 800$ W), gas pressure (2, at 42% He and $w = 800$ W) and input power (3, at 42% He and $p = 10$ mtorr): a) electron temperature; b) electron density; c) total positive ion density; and d) relative density of negative ions

Рис. 1. Параметры электронной и ионной компонент плазмы в зависимости от содержания гелия в плазмообразующем газе (1, при $p = 10$ мторр и $w = 800$ Вт), давления (2, при 42% He и $w = 800$ Вт) и вкладываемой мощности (3, при 42% He и $p = 10$ мторр): а) температура электронов; б) концентрация электронов; в) суммарная концентрация положительных ионов; и д) относительная концентрация отрицательных ионов

An increase in input power under the condition of $y_{\text{He}} > y_{\text{Ar}}$ and $p = \text{const}$ is accompanied by an increase in electron temperature (Fig. 1(a)), electron density (Fig. 1(b)) and total positive ion density (Fig. 1(c)). In our opinion, all three effects are closely connected one with each other and may be explained as follows. From

the input power balance equation [3], it can be understood that the almost direct proportionality between w and n_e values does exist. Physically, the growth of n_e toward higher input powers is provided by an increase in total ionization frequency as well as by limitations of electron loss rates in attachment processes R3-R5.

The latter is due to the acceleration of R6: $SF_x + e \rightarrow SF_{x-1} + F + e$ and R7: $SF_x + e \rightarrow SF_{x-1}^+ + F + 2e$ reaction families that lowers densities of multi-atomic electronegative species and, simultaneously, increases fractions of less saturated radicals and/or atomic by-products. As the corresponding change on plasma composition is characterized by decreasing effective size of dominant neutral species and thus, by lower electron energy losses in both elastic and inelastic collisions, an increase in mean electron energy also takes place. A decrease in plasma electronegativity (Fig. 1(d)) reasonable results from the fasted growth of n_e compared with n_+ , as the latter is «retarded» by decreasing densities of source species for R3-R5.

Fig. 2 shows how variable processing parameters influence emission intensities and densities of fluorine atoms. Obviously, the “raw” intensity data for F 703.8 nm line from Fig. 2(a) has no direct correlation with F atoms density, as represent the combined effect from changes in plasma composition and excitation function, $k_{ex}n_e$, where $k_{ex} = f(T_e)$ is the excitation rate coefficient. At the same time, it is known that the electron-impact excitation of F and Ar atoms is characterized by rather close threshold energies (14.7 eV and 13.5 eV, respectively) while maxima on both cross-sections are located within the electron energy range of 15-20 eV [21]. Such situation causes the nearly constant value of $k_{ex,F}/k_{ex,Ar}$ ratio and finally results in $C_a \approx \text{const}$ at $T_e = 3-6$ eV, as was shown in Ref. [21]. In fact, this means that the parameter I_F/I_{Ar} plotted in Fig. 2(b) adequately traces the relative change of F atom density. In particular, an increase in I_F/I_{Ar} ratio vs. y_{He} exhibits the almost same slope with decreasing y_{Ar} that definitely corresponds to $[F] \approx \text{const}$. Accordingly, the same result in absolute scale is given by Eq. (1), as shown in Fig. 2(c). Though the very weak increasing tendency toward higher y_{He} values can be seen, it is not worth for discussion, as does not exceed the standard experimental error. Physically, such situation is provided by the nearly constant rates of R6 and R7 due to opposite changes of dissociation rate coefficients and electron density (for example, $k_6n_e = 74-87$ s⁻¹ and $k_7n_e = 2.5-5.5$ s⁻¹ for $x = 6$ at 0-46% He).

An increase in gas pressure causes monotonically decreasing I_F/I_{Ar} ratio, but is accompanied by the opposite change in Ar density, $y_{Ar}N$. As a result, the F atom density yielded by Eq. (1) keeps the nearly constant value at $p = 5-15$ mtorr while tends to a weak decrease when gas pressure rises up to 20 mtorr (Fig. 2(c)). The generally similar effect of gas pressure on F atom

density was obtained in Ref. [12] by plasma modeling. In particular, they obtained the weakly increasing $[F]$ value up to ~ 5 mtorr while found the saturation and then, the weakly decreasing region at $p > 15$ mtorr. In our opinion, the reason is that an increase in the density of source SF_x species participating in R6 and R7 is overcompensated by opposite trends for corresponding rate coefficients and n_e . For instance, dissociation frequencies, k_6n_e and k_7n_e , with a participation of SF_6 molecules change as 178-11 s⁻¹ and 10-0.2 s⁻¹, respectively, at $p = 2-20$ mtorr.

An increase in input power causes the rapid increase in both I_F/I_{Ar} ratio and $[F]$ value, as shown in Figs. 2(b) and (c). This quite expectable effect may surely be related to increasing both dissociation degrees for SF_x species and overall production rate of F atoms in R6 and R7 due to the same behavior of electron density. Similar results in both relative and absolute scales have been obtained in Refs. [12, 13] by plasma modeling.

When summarizing above results, one can conclude that effects of gas pressure and input power are quite predictable from general regularities of plasma chemistry. Therefore, the significance of corresponding data is in the confirmation that basic properties of novel $SF_6 + He$ gas system have no principal differences with those reported for SF_6 and $SF_6 + Ar$ plasmas. The more interesting finding reveals that the type of noble additive gas exhibits the noticeable influence on electrons- and ions-related plasma parameters while negligibly affects the F atom density. Therefore, the substitution of Ar by He is expected to provide the stronger influence on ion-driven RIE components (physical sputtering, ion-stimulated desorption of low volatile reaction products, etc.) due to decreasing both ion flux and effective ion mass.

Finally, we would like to focus the attention on the fluorine-atom-to-positive-ion flux ratio, Γ_F/Γ_+ , which characterizes the balance between isotropic and directional etching pathways. As can be seen from Fig. 2(d), this parameter keeps the nearly constant value vs. Ar/He mixing ratio, increases slightly with increasing gas pressure as well as demonstrates the rapid growth toward higher input powers. The latter is because of the faster growth in F atoms density due to the multi-channel formation mechanism for these species in electron-impact processes. Therefore, it can be assumed that the processing conditions providing the maximum etching anisotropy in He-rich plasmas correspond to low pressures and input powers.

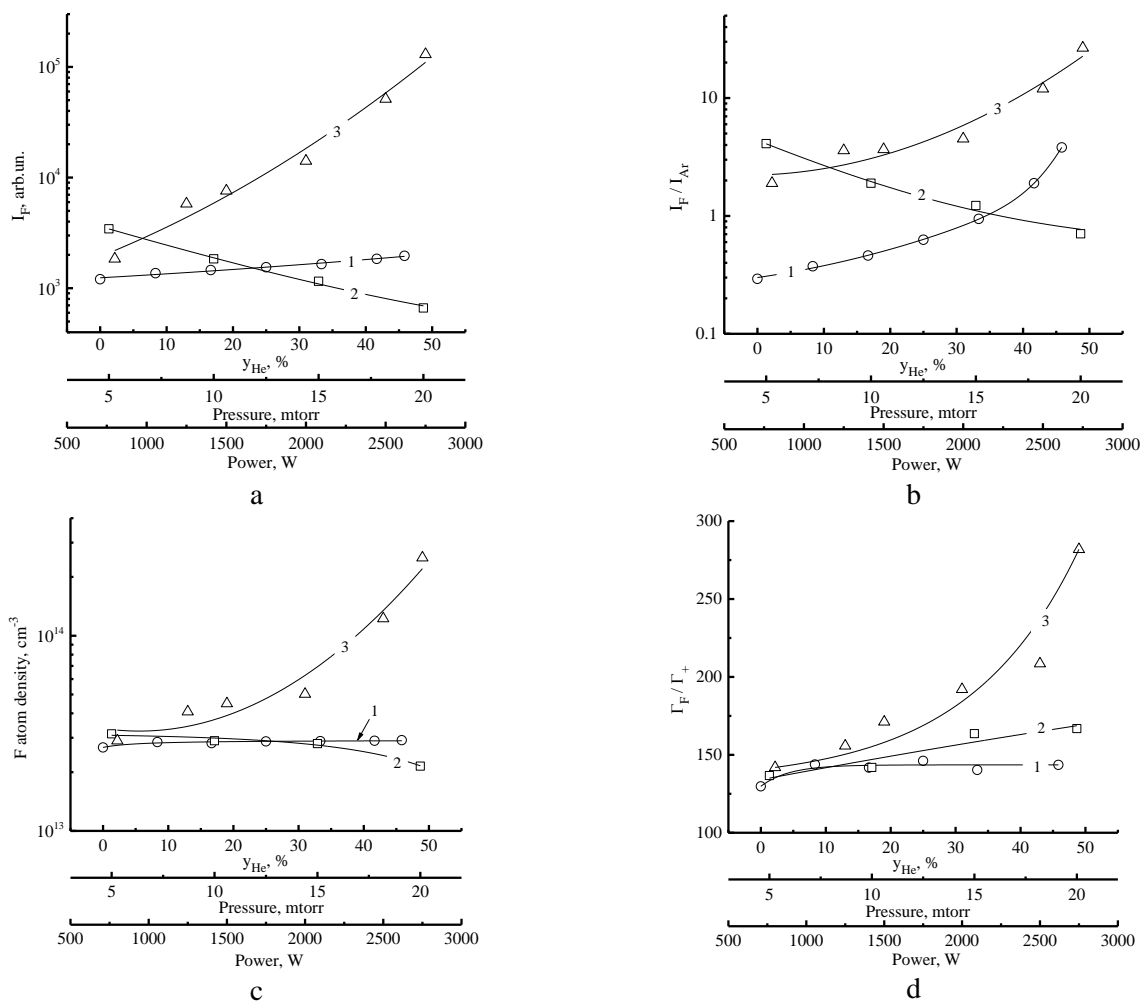


Fig. 2. Emission intensity and density of fluorine atoms as functions of He fraction in a feed gas ($p = 10$ mtorr and $w = 800$ W), gas pressure (2, at 42% He and $w = 800$ W) and input power (3, at 42% He and $p = 10$ mtorr): a) emission intensity for F 703.8 nm line; b) F 703.8 nm / Ar 750.4 nm intensity ratio; c) F atom density provided by actinometry; and d) fluorine-to-positive ion flux ratio, Γ_F/Γ_+ . Рис. 2. Интенсивность излучения и концентрация атомов фтора в зависимости от содержания гелия в плазмообразующем газе (1, при $p = 10$ мторр и $w = 800$ Вт), давления (2, при 42% He и $w = 800$ Вт) и вкладываемой мощности (3, при 42% He и $p = 10$ мторр): а) интенсивность линии F 703.8 нм; б) отношение интенсивностей F 703.8 нм / Ar 750.4 нм; в) концентрация атомов фтора, определенная методом актинометрии; и д) отношение плотностей потоков атомов фтора и положительных ионов, Γ_F/Γ_+ .

CONCLUSIONS

In this work, we investigated the influence of initial mixture composition, gas pressure and input power on physical and chemical properties of $SF_6 + Ar + He$ inductively-coupled plasma under typical reactive-ion etching conditions. For this purpose, we applied plasma diagnostics by Langmuir probes (in order to determine electrons- and ions-related plasma characteristics) and optical emission spectroscopy (in order to determine F atom density using the actinometry procedure). The combination of these data allowed one to investigate for the first time the effect of Ar/He mixing ratio, to confirm the influence of gas pressure and input power known from previous works as well as to suggest mechanisms responsible for obtained phenomena. In particular, it can be concluded that the substitution

of argon by helium at constant SF_6 content in a feed gas affects the electron temperature, densities of charged species and plasma electronegativity through changes in both total ionization rate and electron energy losses. It was shown also that the maximum effect on the F atom density belongs to input power while the influence of both Ar/He ratio and gas pressure is limited by opposite changes in electron temperature and electron density. In He-rich plasmas, the minimum of fluorine atom-to-positive ion flux ratio characterizing the balance between chaotic and directional etching pathways corresponds to low pressures and input powers.

The work was supported by the Russian Science Foundation grant No. 24-69-00039, <https://rscf.ru/en/project/24-69-00039/>.

The authors declare the absence of a conflict of interest warranting disclosure in this article.

Исследование выполнено за счет средств гранта Российского научного фонда No. 24-69-00039, <https://rscf.ru/project/24-69-00039/>.

Авторы заявляют об отсутствии конфликта интересов, требующего раскрытия в данной статье.

REFERENCES ЛИТЕРАТУРА

1. **Nojiri K.** Dry etching technology for semiconductors. Tokyo: Springer Internat. Publ. 2015. 116 p. DOI: 10.1007/978-3-319-10295-5.
2. **Wolf S., Tauber R.N.** Silicon Processing for the VLSI Era. Volume 1. Process Technology. New York: Latt. Press. 2000. 416 p.
3. **Lieberman M.A., Lichtenberg A.J.** Principles of plasma discharges and materials processing. New York: John Wiley & Sons Inc. 2005. 757 p. DOI: 10.1002/0471724254.
4. **Donnelly V.M., Kornblit A.** Plasma etching: Yesterday, today, and tomorrow. *J. Vac. Sci. Technol.* 2013. V. 31. P. 050825-48. DOI: 10.1116/1.4819316.
5. **Kastenmeier B.E.E., Matsuo P.J., Oehrlein G.S.** Highly selective etching of silicon nitride over silicon and silicon dioxide. *J. Vac. Sci. Technol. A.* 1999. V. 17. P. 3179-3184. DOI: 10.1116/1.58209.
6. **Schaepkens M., Standaert T.E.F.M., Rueger N.R., Sebel P.G.M., Oehrlein G.S., Cook J.M.** Study of the SiO₂-to-Si₃N₄ etch selectivity mechanism in inductively coupled fluorocarbon plasmas and a comparison with the SiO₂-to-Si mechanism. *J. Vac. Sci. Technol. A.* 1999. V. 17. P. 26-37. DOI: 10.1116/1.582108.
7. **Standaert T.E.F.M., Hedlund C., Joseph E.A., Oehrlein G.S., Dalton T.J.** Role of fluorocarbon film formation in the etching of silicon, silicon dioxide, silicon nitride, and amorphous hydrogenated silicon carbide. *J. Vac. Sci. Technol. A.* 2004. V. 22. P. 53-60. DOI: 10.1116/1.1626642.
8. **Oehrlein G.S.** Future of plasma etching for microelectronics: Challenges and opportunities. *J. Vac. Sci. Technol. B.* 2024. V. 42. P. 041501. DOI: 10.1116/6.0003579.
9. **Dussart R., Tillocher T., Lefauchaux P., Boufnichel M.** Plasma cryogenic etching of silicon: from the early days to today's advanced technologies. *J. Phys. D: Appl. Phys.* 2014. V. 47. P. 123001. DOI: 10.1088/0022-3727/47/12/123001.
10. **Rudenko M.K., Myakon'kikh A.V., Lukichev V.F.** Monte Carlo simulation of defects of a trench profile in the process of deep reactive ion etching of silicon. *Russ. Microelectr.* 2019. V. 48. N 3. P. 157-166. DOI: 10.1134/S1063739719030090.
11. **Yoon S.F.** Dry etching of thermal SiO₂ using SF₆-based plasma for VLSI fabrication. *Microelectr. Eng.* 1991. V. 14. N 1. P. 23-40. DOI: 10.1016/0167-9317(91)90164-9.
12. **Kokkoris G., Panagiotopoulos A., Goodyear A., Cooke M., Gogolides E.** A global model for SF₆ plasmas coupling reaction kinetics in the gas phase and on the surface of the reactor walls. *J. Phys. D: Appl. Phys.* 2009. V. 42. P. 055209. DOI: 10.1088/0022-3727/42/5/055209.
13. **Mao M., Wang Y.N., Bogaerts A.** Numerical study of the plasma chemistry in inductively coupled SF₆ and SF₆/Ar plasmas used for deep silicon etching applications. *J. Phys. D: Appl. Phys.* 2011. V. 44. P. 435202. DOI: 10.1088/0022-3727/44/43/435202.
14. **Lallement L., Rhallabi A., Cardinaud C., Peignon-Fernandez M.C., Alves L.L.** Global model and diagnostic of a low-pressure SF₆/Ar inductively coupled plasma. *Plasma Sources Sci. Technol.* 2009. V. 18. P. 025001. DOI: 10.1088/0963-0252/18/2/025001.
15. **Rauf S., Ventzek P.L.G., Abraham I.C., Hebner G.A., Woodworth J.R.** Charged species dynamics in an inductively coupled Ar/SF₆ plasma discharge. *J. Appl. Phys.* 2002. V. 92. N 12. P. 6998-7007. DOI: 10.1063/1.1519950.
16. Handbook of Chemistry and Physics. New York: CRC Press. 2023. 1580 p.
17. **Chiad B.T., Al-Zubaydi T.L., Khalaf M.K., Khudiar A.I.** Characterization of low pressure plasma dc discharges (Ar, SF₆ and SF₆/He) for Si etching. *Indian J. Pure Appl. Phys.* 2010. V. 48. P. 723-730.
18. **Rezvanov A., Miakonkikh A.V., Vishnevskiy A.S., Rudenko K.V., Baklanov M.R.** Cryogenic etching of porous low-k dielectrics in CF₃Br and CF₄ plasmas. *J. Vac. Sci. Technol. B.* 2017. V. 35. P. 021204.
19. **Miakonkikh A., Kuzmenko V., Efremov A., Rudenko K.** A comparison of CF₄, CBrF₃ and C₂Br₂F₄ Plasmas: Physical Parameters and Densities of Atomic Species. *Vacuum.* 2022. V. 200. P. 110991. DOI: 10.1016/j.vacuum.2022.110991.
20. **Shun'ko E.V.** Langmuir probe in theory and practice. Boca Raton: Universal Publ. 2008. 245 p.
21. **Lopaev D.V., Volynets A.V., Zyryanov S.M., Zotovich A.I., Rakhimov A.T.** Actinometry of O, N and F atoms. *J. Phys. D: Appl. Phys.* 2017. V. 50. P. 075202. DOI: 10.1088/1361-6463/50/7/075202.
22. **Cunge G., Ramos R., Vempaire D., Touzeau M., Neijbauer M., Sadeghi N.** Gas temperature measurement in CF₄, SF₆, O₂, Cl₂ and HBr inductively coupled plasmas. *J. Vac. Sci. Technol. A.* 2009. V. 27. P. 471-478. DOI: 10.1116/1.3106626.
23. **Ефремов А.М., Бобылев А.В., Кwon К.-Н.** Параметры плазмы и кинетика травления кремния в смеси CF₄ + C₄F₈ + O₂: эффект соотношения CF₄/C₄F₈. *Изв. вузов. Химия и хим. технология.* 2024. Т. 67. Вып. 6. С. 29-37. **Ефремов А.М., Бобылев А.В., Кwon К.-Н.** Plasma parameters and silicon etching kinetics in CF₄ + C₄F₈ + O₂ mixture: effect of CF₄/C₄F₈ mixing ratio. *ChemChemTech [Izv. Vyssh. Uchebn. Zaved. Khim. Tekhnol.]*. 2024. V. 67. N 6. P. 29-37. DOI: 10.6060/ivkkt.20246706.6982.
24. **Ефремов А.М., Башмакова Д.Е., Кwon К.-Н.** Особенности состава плазмы и кинетики атомов фтора в смеси CHF₃ + O₂. *Изв. вузов. Химия и хим. технология.* 2023. Т. 66. Вып. 1. С. 48-55. **Ефремов А.М., Башмакова Д.Е., Кwon К.-Н.** Features of plasma composition and fluorine atom kinetics in CHF₃ + O₂ gas mixture. *ChemChemTech [Izv. Vyssh. Uchebn. Zaved. Khim. Tekhnol.]*. 2023. V. 66. N 1. P. 48-55. DOI: 10.6060/ivkkt.20236601.6667.
25. **Raju G.G.** Gaseous electronics. Tables, Atoms and Molecules. Boca Raton: CRC Press. 2012. 790 p. DOI: 10.1201/b11492.
26. **Christophorou L.G., Olthoff J.K.** Fundamental electron interactions with plasma processing gases. New York: Springer Science+Business Media LLC. 2004. 776 p. DOI: 10.1007/978-1-4419-8971-0.

Поступила в редакцию (Received) 20.08.2024

Принята к опубликованию (Accepted) 03.10.2024